

Introduction to Geophysical Fluid Dynamics

Physical and Numerical Aspects
Second Edition

Benoit Cushman-Roisin
Thayer School of Engineering
Dartmouth College
Hanover, New Hampshire 03755
USA

Jean-Marie Beckers
Département d'Astrophysique,
Géophysique et Océanographie
Université de Liège
B-4000 Liège
Belgium



AMSTERDAM • BOSTON • HEIDELBERG • LONDON
NEW YORK • OXFORD • PARIS • SAN DIEGO
SAN FRANCISCO • SINGAPORE • SYDNEY • TOKYO

Academic Press is an imprint of Elsevier



grid points,⁸ avoidance of aliasing requires the use of $(3M + 1)$ evaluation points in longitude. Hence a model with 42 modes will use typically an underlying longitude–latitude grid of 128×64 points for the evaluation of the nonlinear terms (note the rounding toward powers of 2 to take advantage of efficient FFTs). This grid is called the *Gaussian grid* or *transform grid*. The calculation of grid spacing based on the number of Gaussian grid points overestimates actual resolution because it is designed to avoid aliasing on nonlinear interactions, and the actual, lower resolution is that which corresponds to the wavenumbers associated with the spectral decomposition.

The transform methods thus allows us to calculate some terms in spectral space (linear terms) and others (quadratic advection terms and nonlinear terms stemming from various parameterizations) in the transformed space so as to use the most appropriate technique for each term. In practice, it means that the model utilizes both spectral and grid representations of each variable.

The high convergence rate of spectral methods is inherited with the spherical harmonics, as long as the physical solution is sufficiently smooth. When fronts or jumps are present in the solution, however, spatial oscillations emerge near the place of rapid variation. This is known as Gibb's phenomena. The associated over- or undershooting on the physical grid can lead to spurious physical results. An overshooting of specific humidity, for example, may lead to the poetically named *spectral rain*.

Because of the calculation of some terms on the physical grid, the geometrical convergence of meridians toward the poles may also be a problem. For the advection part, this can be overcome by the semi-Lagrangian approach, which we describe next.

19.8 SEMI-LAGRANGIAN METHODS

To deal with advection, we again turn our attention to the passive-tracer concentration c , which is conserved along a trajectory of a parcel of fluid as long as diffusion remains negligible. The Lagrangian approach ensures exact conservation of the tracer value at the price of calculating its trajectory in time (see Section 12.8). As we have seen, however, the pure Lagrangian method leads sooner or later to an impractical distribution of particles, and it becomes impossible to determine concentration values in regions nearly void of particles. This is what happens when we follow the same set of particles over time: some of which flow out of the system or are caught in stagnation points. *Semi-Lagrangian* methods avoid this problem by using a different set of particles at each time step. The set is chosen at t^n so that at t^{n+1} the chosen particles arrive at the nodes of the numerical grid. This amounts to integrating trajectories

⁸Remember that the sum runs from $-M$ to M .

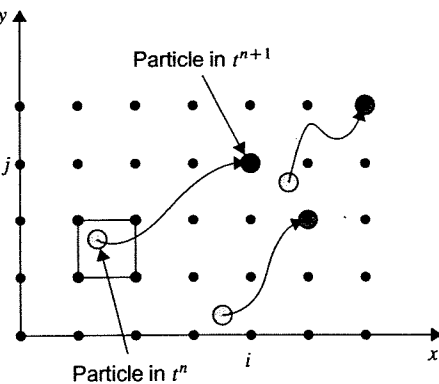


FIGURE 19.11 In a semi-Lagrangian method, trajectories are integrated backward in order to find an earlier location of the fluid particle that reaches grid node (i, j) by time t^{n+1} . Once this location is known, the value of the variable of interest, such as a temperature or concentration, at that location can be obtained by interpolation of nearby values. The interpolated value is then translated by advection to the new location (i, j) at time t^{n+1} .

backward for one time step in order to find where they originate. Once the past locations are determined, at t^n , the concentration in those locations is then determined by interpolation among known values on the grid (Fig. 19.11).

For simplification, let us consider first the one-dimensional case with positive velocity u and uniformly spaced grid (Fig. 19.12). The particle that lands at grid node x_i by time t^{n+1} was at the earlier time $t^n = t^{n+1} - \Delta t$ at position

$$x = x_i - u\Delta t. \quad (19.29)$$

On a uniform grid with spacing Δx , this position x most likely lies within a grid interval rather than, per chance, at an other grid point. This grid interval is given by

$$x_{i-1-p} \leq x = x_i - u\Delta t \leq x_{i-p}, \quad \text{with } p = \text{integer part of } u \frac{\Delta t}{\Delta x}. \quad (19.30)$$

By virtue of advection without diffusion, the value of \tilde{c}_i^{n+1} is none other than \tilde{c}^n at x , a value which we can obtain by interpolation. Performing a linear interpolation, we obtain

$$\tilde{c}_i^{n+1} = \frac{(x_{i-p} - x)}{\Delta x} \tilde{c}_{i-1-p}^n + \frac{(x - x_{i-1-p})}{\Delta x} \tilde{c}_{i-p}^n = \tilde{C} \tilde{c}_{i-1-p}^n + (1 - \tilde{C}) \tilde{c}_{i-p}^n, \quad (19.31)$$

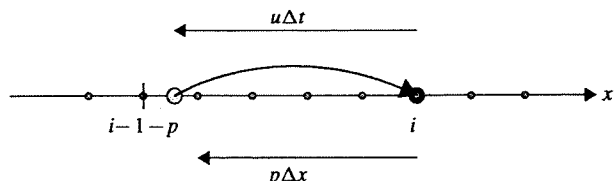


FIGURE 19.12 The semi-Lagrangian method in one dimension. The particle in light gray moves during time interval $[t^n, t^{n+1}]$ over a distance $u\Delta t$ to reach grid node labeled i at time t^{n+1} .

for which we define

$$\tilde{C} = \left(\frac{u\Delta t}{\Delta x} - p \right). \quad (19.32)$$

The scheme is monotonic and thus of first order. We can easily see that, as long as $u\Delta t \leq \Delta x$ (and thus $p = 0$), the scheme is equivalent to the upwind scheme. However, contrary to the upwind scheme, no stability condition is necessary here because the method uses the correct grid interval from which to interpolate. Numerical diffusion persists, however, although it is reduced in the sense that large time steps can be used and the total number of time steps can be decreased. For a given simulation time, fewer time steps mean less numerical diffusion.

To decrease the amount of diffusion introduced by the interpolation, a better than linear interpolation can be used. A second-order, parabolic interpolation yields a scheme equivalent to the Lax–Wendroff method.⁹

In two dimensions, the approach is readily generalized with backward trajectories for a single time step followed by 2D spatial interpolation (either bilinear or biparabolic). The trajectory calculation needs to take into account that the flow field (u, v) , and this may become quite complicated if $U\Delta t \geq \Delta x$. If the velocity field varies over the trajectory on a scale comparable to the grid scale Δx , intermediate time steps are necessary for the calculation of the backward trajectory in order to maintain accuracy, and the calculation cost increases rapidly.

However, if the velocity is relatively smooth on the scale of the numerical grid (which ought to be the case and will necessarily be the case near the pole), that is, $\Delta x \ll L$, simple trajectory integrations will suffice. In fact, if $\Delta x \ll U\Delta t \ll L$ the semi-Lagrangian approach is much more efficient than the Eulerian method because during each time step, a large number of grid points can be “jumped over” by advection. Hence, interpolation (and associated diffusion) is less frequent, and the spatial scale of the trajectories is correctly captured. This is the way to reap the maximum benefit for the Semi-Lagrangian approach.

If $\Delta x \sim L$, time steps are similar to the Eulerian approach. The major advantage in this case is the stability of the method in the face of the occasionally excessive time step. For higher accuracy, however, one should not use longer time steps than allowed by $U\Delta t \sim L$. If there are many different tracers to be advected simultaneously, as in air pollution studies or ecosystem modeling, the method presents considerable advantages because a single, common trajectory needs to be calculated for all tracers.

For the nonadvective terms, such as source/sink and diffusion terms, a fractional-step approach is possible, for example, by first using a semi-

⁹Note the difference: In Eulerian methods, we spoke about interpolating for flux calculations to be discretized subsequently; here we speak about interpolation of the solution itself.

Lagrangian advection scheme followed by a Eulerian diffusion scheme either on the physical grid or in spectral space. Alternatively, the evolution of source terms may be taken into account along the trajectory (e.g., McDonald, 1986). Contrary to the finite-volume approach of Eulerian methods, global conservation properties are more difficult to handle but can be respected (e.g., Yabe, Xiao & Utsumi, 2001).

ANALYTICAL PROBLEMS

- 19.1. Consider the regular gardening greenhouse and idealize the system as follows: The air plays no role, the ground absorbs all radiation and reradiates it as a black body, and the glass is perfectly transparent to short-wave (visible) radiation but totally opaque to long-wave (heat) radiation. Further, the glass emits its radiation inward and outward in equal parts. Compare the ground temperature inside the greenhouse with that outside. Then, redo the exercise for a greenhouse with two layers of glass separated by a layer of air.
- 19.2. Consider the long-wave radiation fluxes of Figs. 19.2 and 19.3. In each case, the upward flux from the ground (E_2) is greater than the downward flux from the atmosphere ($0.64 E_1$). Can you explain why?
- 19.3. Consider the crudest heat budget for the earth (without atmosphere and hydrological cycle) and assume the following dependency of the albedo on temperature: At low temperatures, much ice and clouds cover the earth, yielding a high albedo, whereas at high temperatures, the absence of ice and clouds reduce the albedo to zero. Taking the functional dependence as

$$\begin{aligned}\alpha &= 0.5 \quad \text{for } T \leq 250 \text{ K} \\ \alpha &= \frac{270 - T}{40} \quad \text{for } 250 \text{ K} \leq T \leq 270 \text{ K} \\ \alpha &= 0 \quad \text{for } 270 \text{ K} \leq T,\end{aligned}\tag{19.33}$$

solve for the earth's average temperature T . Discuss the several solutions.

- 19.4. Using the global heat budget of the earth model, complete with an atmospheric layer and hydrological cycle, explore a worst-case scenario, whereby elevated concentrations of greenhouse gases completely block the transmission of long-wave radiation from the earth's surface, the intensity of the hydrological cycle is unchanged, and the anticipated global warming has caused the complete melting of all ice sheets, effectively eliminating all reflection by the earth's surface of short-wave solar radiation. What would then be the globally averaged temperature of the earth's surface? (Except for those transmission and reflection coefficients that need to be revised, use the parameter values quoted in the text.)

NUMERICAL EXERCISES

- 19.1. What is the spatial resolution (in kilometers) along the equator for a T256 spectral model? How many grid points must the underlying Gaussian grid have in order to avoid aliasing in the advection terms?
- 19.2. Use `spherical.m` to consider other basis functions $Y_{m,n}$ than those of Fig. 19.9.
- 19.3. Estimate the numerical cost of the forward and inverse transform associated with spectral harmonics.
- 19.4. In addition to the problem of decreasing grid spacing near the poles, which other problem can you identify at the poles for models that do not work with a spectral decomposition? (*Hint:* Think about boundary conditions for an AGCM, for longitude first and then for latitude.)
- 19.5. Exploiting properties of Legendre polynomials, given for example in Abramowitz and Stegun (1972), find the spectral coefficients of spatial derivatives, knowing the spectral coefficients of the function to be differentiated.

In an Eulerian reference frame, the observer remains at a fixed position in space.



Eulerian framework

In an Eulerian reference frame, the observer remains at a fixed position in space.



Eulerian framework

In an Eulerian reference frame, the observer remains at a fixed position in space.

$$\frac{\partial Q}{\partial t} + \vec{u} \cdot \nabla Q = 0$$

where $\vec{u} = d\vec{x}/dt$



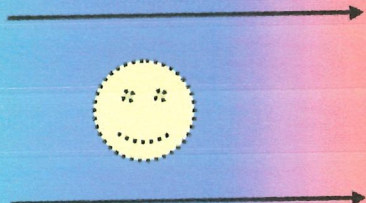
Eulerian framework

In a Lagrangian reference frame, the observer moves with the fluid.



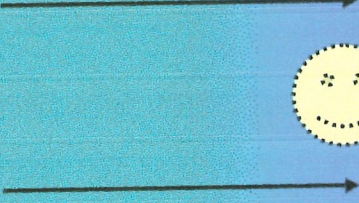
Lagrangian framework

In a Lagrangian reference frame, the observer moves with the fluid.



Lagrangian framework

In a Lagrangian reference frame, the observer moves with the fluid.



Lagrangian framework

In a Lagrangian reference frame, the observer moves with the fluid.

$$\frac{dQ}{dt} = 0$$

Lagrangian framework

Example: 1D advection equation

Continuous form:

$$\frac{dQ}{dt} = \frac{\partial Q}{\partial t} + U(x, t) \frac{\partial Q}{\partial x} = 0$$

Eulerian finite-difference

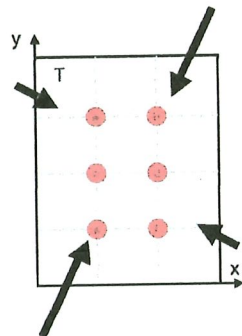
$$\frac{Q_i(t + \Delta t) - Q_i(t - \Delta t)}{2\Delta t} + U_i(t) \frac{Q_{i+1}(t) - Q_{i-1}(t)}{2\Delta x} = 0$$

Traditional semi-Lagrangian

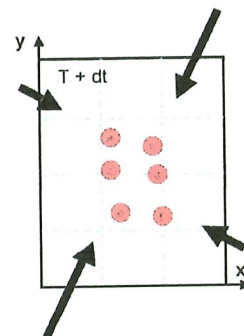
$$\frac{Q_i(t + \Delta t) - Q_D(t - \Delta t)}{2\Delta t} = 0$$

What does “semi”-Lagrangian mean?

In a fully-Lagrangian model, we would be following every parcel throughout the simulation.

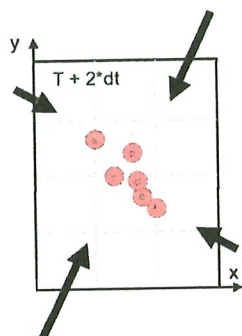


In a fully-Lagrangian model, we would be following every parcel throughout the simulation.



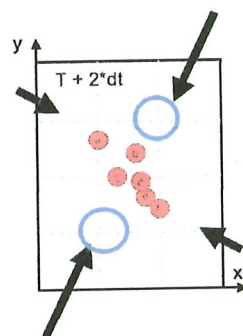
What does “semi”-Lagrangian mean?

In a fully-Lagrangian model, we would be following every parcel throughout the simulation.



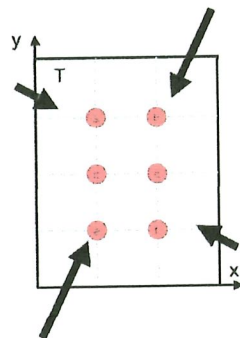
What does “semi”-Lagrangian mean?

But parts of the domain will be under-resolved if the parcels end up in clusters.



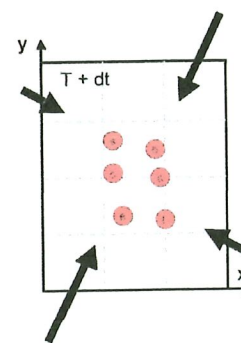
What does "semi"-Lagrangian mean?

As a remedy, instead of strictly tracking each parcel time step after time step, we only follow each parcel over one time step, after which, the parcels are reset back to the Eulerian grid. Thus, the term "semi"-Lagrangian.



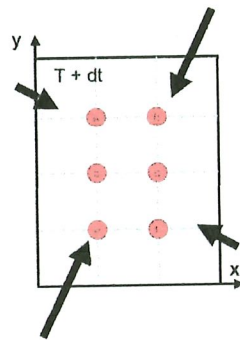
What does "semi"-Lagrangian mean?

As a remedy, instead of strictly tracking each parcel time step after time step, we only follow each parcel over one time step, after which, the parcels are reset back to the Eulerian grid. Thus, the term "semi"-Lagrangian.



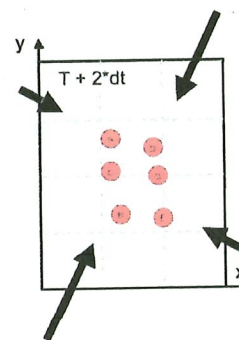
What does "semi"-Lagrangian mean?

As a remedy, instead of strictly tracking each parcel time step after time step, we only follow each parcel over one time step, after which, the parcels are reset back to the Eulerian grid. Thus, the term "semi"-Lagrangian.



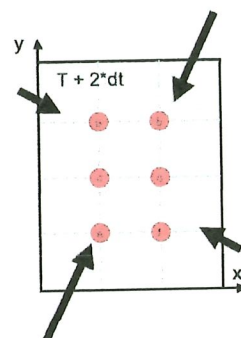
What does "semi"-Lagrangian mean?

As a remedy, instead of strictly tracking each parcel time step after time step, we only follow each parcel over one time step, after which, the parcels are reset back to the Eulerian grid. Thus, the term "semi"-Lagrangian.



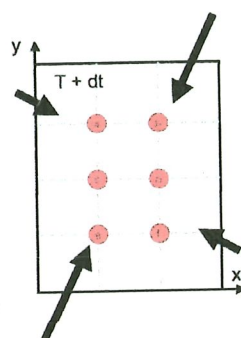
What does "semi"-Lagrangian mean?

As a remedy, instead of strictly tracking each parcel time step after time step, we only follow each parcel over one time step, after which, the parcels are reset back to the Eulerian grid. Thus, the term "semi"-Lagrangian.



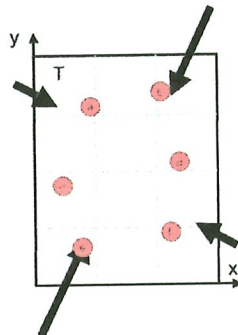
What does "semi"-Lagrangian mean?

Instead of computing forward trajectories, we can also compute backward trajectories and reset the parcels at the arrival time-level back onto the Eulerian grid.



What does "semi"-Lagrangian mean?

Instead of computing *forward trajectories*, we can also compute *backward trajectories* and reset the parcels at the arrival time-level back onto the Eulerian grid.



Stability condition in Eulerian schemes

Recall that the Courant-Friedrichs-Lowy (CFL) condition "requires that the numerical domain of dependence of a finite-difference scheme include the domain of dependence of the associated partial differential equation."

(Durran, 2010)

Courant-Friedrichs-Lowy (CFL) stability condition:

$$C = \frac{\sqrt{N}|v|\Delta t}{\Delta x} \leq 1$$

where Δt is the time step, Δx is the grid spacing, and $|v|$ is the maximum advection speed.

Semi-Lagrangian schemes use a regular grid (like the Eulerian scheme), but has the numerical stability of a Lagrangian scheme.

Semi-Lagrangian schemes use a regular grid (like the Eulerian scheme), but has the numerical stability of a Lagrangian scheme.

These schemes consist of two main steps:

- 1) computation of the backward trajectories
- 2) computation of the value at the departure time-level

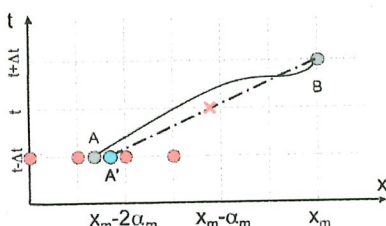
Computation of the departure value

Trajectory computation

$$\alpha_m = \Delta t \cdot U(x_m - \alpha_m, t)$$

Iterate to get $U(x_m - \alpha_m, t)$ (converges typically at 3 iterations)

Grid-point interpolation



Limitations of traditional semi-Lagrangian methods

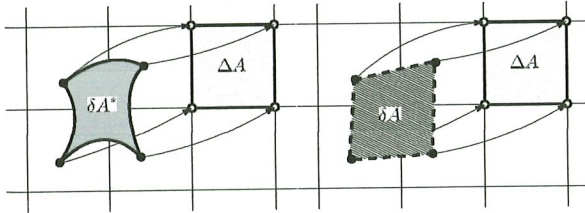
- grid-point interpolation introduces damping
- requires a posteriori mass fixers to conserve mass

This pitfall has led to the development of inherently-conservative semi-Lagrangian schemes, e.g. flux-form versions (Laprise and Plante, 1995; Lin and Rood, 1996; Harris et al. 2011), and cell-integrated versions (Rančić, 1992; Nair and Machenhauer, 2002; Zerroukat et al., 2002; Lauritzen et al. 2010).

Conserving mass using a CISL scheme — CSLAM

Cell-integrated semi-Lagrangian (CISL) schemes are inherently mass-conserving.

We utilize the Conservative Semi-Lagrangian Multi-tracer (CSLAM) transport scheme (Lauritzen et al., 2010).

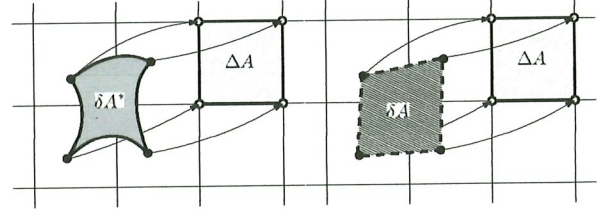


31 / 85

Conserving mass using a CISL scheme — CSLAM

$$\text{Continuous } \frac{\partial \rho}{\partial t} + \nabla \cdot (\rho \mathbf{v}) = 0$$

$$\text{CSLAM } \bar{\rho}_{\text{exp}}^{n+1} \Delta A = \bar{\rho}_*^n \delta A \text{ where } \bar{\rho}_*^n = \frac{1}{\delta A} \iint_{\delta A} \rho^n(x, y) dA$$

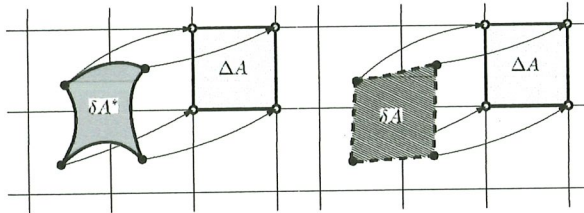


32 / 85

Conserving mass using a CISL scheme — CSLAM

$$\text{Continuous } \frac{\partial \rho q_j}{\partial t} + \nabla \cdot (\rho q_j \mathbf{v}) = 0$$

$$\text{CSLAM } \bar{\rho} q_j^{n+1} \Delta A = \bar{\rho} q_j^n \delta A \text{ where } \bar{\rho} q_j^n = \frac{1}{\delta A} \iint_{\delta A} \rho q_j^n(x, y) dA$$



33 / 85

34 / 85

A cell-integrated semi-Lagrangian semi-implicit solver

Governing equations for a shallow-water system:

$$\frac{\partial u}{\partial t} + u \frac{\partial u}{\partial x} + v \frac{\partial u}{\partial y} - g \frac{\partial h}{\partial x} = 0$$

$$\frac{\partial v}{\partial t} + u \frac{\partial v}{\partial x} + v \frac{\partial v}{\partial y} - g \frac{\partial h}{\partial y} = 0$$

$$\frac{\partial h}{\partial t} + \nabla \cdot (h \mathbf{v}) = 0$$

$$\frac{\partial(hq)}{\partial t} + \nabla \cdot (hq \mathbf{v}) = 0$$

A cell-integrated semi-Lagrangian semi-implicit solver

$$\frac{\partial u}{\partial t} + u \frac{\partial u}{\partial x} + v \frac{\partial u}{\partial y} - g \frac{\partial h}{\partial x} = 0$$

$$\frac{\partial v}{\partial t} + u \frac{\partial v}{\partial x} + v \frac{\partial v}{\partial y} - g \frac{\partial h}{\partial y} = 0$$

$$\left[\frac{du}{dt} \right] - g \frac{\partial h}{\partial x} = 0$$

$$\left[\frac{dv}{dt} \right] - g \frac{\partial h}{\partial y} = 0$$

35 / 85

36 / 85

A cell-integrated semi-Lagrangian semi-implicit solver

A cell-integrated semi-Lagrangian semi-implicit solver

$$\frac{du}{dt} - \left[g \frac{\partial h}{\partial x} \right] = 0 \quad (\text{implicit})$$

$$\frac{dv}{dt} - \left[g \frac{\partial h}{\partial y} \right] = 0 \quad (\text{implicit})$$

$$\frac{du}{dt} - g \frac{\partial h}{\partial x} = 0$$

$$\frac{dv}{dt} - g \frac{\partial h}{\partial y} = 0$$

Forward-in-time:

$$u_A^{n+1} = u_D^n + \Delta t \left(\frac{1-\beta}{2} \right) \left[-g \delta_x h \right]_D^n + \Delta t \left(\frac{1+\beta}{2} \right) \left[-g \delta_x h \right]_A^{n+1}$$

$$v_A^{n+1} = v_D^n + \Delta t \left(\frac{1-\beta}{2} \right) \left[-g \delta_y h \right]_D^n + \Delta t \left(\frac{1+\beta}{2} \right) \left[-g \delta_y h \right]_A^{n+1}$$

where β is a time-off-centering parameter.

27 / 65

22 / 65

Semi-implicit CISL continuity equation (Lauritzen et al., 2006):

$$\frac{\partial h}{\partial t} + \nabla \cdot (h \mathbf{v}) = 0$$

$$h_A^{n+1} = h_{\text{exp}}^{n+1} - \frac{\Delta t}{2} H_0 \left[\boxed{\nabla_{\text{eul}} \cdot \mathbf{v}^{n+1}} - \nabla_{\text{lag}} \cdot \tilde{\mathbf{v}}^{n+1} \right]$$

(coupled to the momentum equations)

A cell-integrated semi-Lagrangian semi-implicit solver

Forward-in-time:

$$u_A^{n+1} = u_D^n + \Delta t \left(\frac{1-\beta}{2} \right) \left[-g \delta_x h \right]_D^n + \Delta t \left(\frac{1+\beta}{2} \right) \left[-g \delta_x h \right]_A^{n+1}$$

$$v_A^{n+1} = v_D^n + \Delta t \left(\frac{1-\beta}{2} \right) \left[-g \delta_y h \right]_D^n + \Delta t \left(\frac{1+\beta}{2} \right) \left[-g \delta_y h \right]_A^{n+1}$$

Semi-implicit CISL continuity equation (Lauritzen et al., 2006):

$$h_A^{n+1} = h_{\text{exp}}^{n+1} - \frac{\Delta t}{2} H_0 \left[\boxed{\nabla_{\text{eul}} \cdot \mathbf{v}^{n+1}} - \nabla_{\text{lag}} \cdot \tilde{\mathbf{v}}^{n+1} \right]$$

(coupled to the momentum equations)

36 / 65

40 / 65

A cell-integrated semi-Lagrangian semi-implicit solver

Helmholtz equation:

$$h_A^{n+1} + A \delta_{xx} h_A^{n+1} + B \delta_{yy} h_A^{n+1} = \text{R.H.S.}$$

where the only unknown is h_A^{n+1} and the equation is solved iteratively, e.g. using a conjugate gradient method.

Then, compute u^{n+1}, v^{n+1} using h_A^{n+1} solutions.

Algorithm for a SLSI solver using CISL schemes

1. Form discretized semi-implicit system
2. Use CISL scheme (e.g. CSLAM) to get h_{exp}^{n+1}
3. Solve the linear Helmholtz equation for h_A^{n+1}
4. Solve for u, v using h_A^{n+1} solutions
5. Compute prognostic variable $h q^{n+1}$ & diagnostic variable q^{n+1}

$$\text{Example: } u_A^{n+1} = \frac{\Delta t}{2} \left[-g' \delta_x h \right]_A^{n+1} + R_u^n,$$

$$v_A^{n+1} = \frac{\Delta t}{2} \left[-g' \delta_y h \right]_A^{n+1} + R_v^n.$$

$$h_A^{n+1} = h_{\text{exp}}^{n+1} - \frac{\Delta t}{2} H_0 \left[\nabla_{\text{eul}} \cdot \mathbf{v}^{n+1} - \nabla_{\text{lag}} \cdot \tilde{\mathbf{v}}^{n+1} \right]$$

$$\text{Helmholtz equation: } h_A^{n+1} + A \delta_{xx} h_A^{n+1} + B \delta_{yy} h_A^{n+1} = \text{R.H.S.}$$

$$\text{Prognostic: } h q_A^{n+1} = h q_{\text{exp}}^{n+1}$$

$$\text{Diagnostic: } q^{n+1} = h q^{n+1} / h^{n+1}$$

41 / 65

42 / 65

Conservative tracer transport

Desirable to maintain consistency between the discrete equations of:
(example: SW system)

$$\frac{\partial h}{\partial t} + \nabla \cdot (h\mathbf{v}) = 0 \quad (1)$$

$$\frac{\partial(hq)}{\partial t} + \nabla \cdot (hq\mathbf{v}) = 0 \quad (2)$$

Numerical consistency

When $q = 1$, discrete scheme for (2) should reduce to that for (1). The lack of numerical consistency between the continuity equation and the scalar conservation equation can lead to the unphysical generation or removal of model constituent mass.
→ "consistent tracer transport" or "free-stream preserving"

Lack of consistency in a semi-implicit system

Discrete semi-implicit CISL continuity equation (Lauritzen et al. 2006) [LKM]

$$h^{n+1} = \bar{h}_{\text{exp}}^{n+1} - \frac{\Delta t}{2} H_0 [\nabla_{\text{eul}} \cdot \mathbf{v}^{n+1} - \nabla_{\text{lag}} \cdot \tilde{\mathbf{v}}^{n+1}] + \frac{\Delta t}{2} H_0 [\nabla_{\text{eul}} \cdot \mathbf{v}^n - \nabla_{\text{lag}} \cdot \mathbf{v}^n] \frac{\delta A^*}{\Delta A}$$

where $\bar{[]}$ refers to the cell-averaged value.

Explicitly solve for $\bar{h}q^{n+1}$ using CSLAM

$$\bar{h}q^{n+1} = \bar{h}q_{\text{exp}}^{n+1}$$

Lack of consistency in a semi-implicit system

Discrete semi-implicit CISL continuity equation (Lauritzen et al. 2006) [LKM]

$$h^{n+1} = \bar{h}_{\text{exp}}^{n+1} - \frac{\Delta t}{2} H_0 [\nabla_{\text{eul}} \cdot \mathbf{v}^{n+1} - \nabla_{\text{lag}} \cdot \tilde{\mathbf{v}}^{n+1}] + \frac{\Delta t}{2} H_0 [\nabla_{\text{eul}} \cdot \mathbf{v}^n - \nabla_{\text{lag}} \cdot \mathbf{v}^n] \frac{\delta A^*}{\Delta A}$$

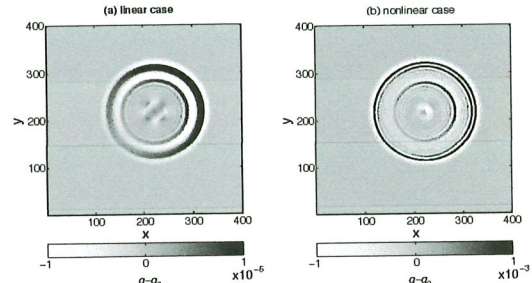
where $\bar{[]}$ refers to the cell-averaged value.

Consistent scalar transport using LKM

$$\bar{h}q^{n+1} = \bar{h}q_{\text{exp}}^{n+1} + \frac{\Delta t}{2} H Q_0 [\nabla_{\text{eul}} \cdot \mathbf{v}^n - \nabla_{\text{lag}} \cdot \mathbf{v}^n] \frac{\delta A^*}{\Delta A} - \frac{\Delta t}{2} H Q_0 [\nabla_{\text{eul}} \cdot \mathbf{v}^{n+1} - \nabla_{\text{lag}} \cdot \tilde{\mathbf{v}}^{n+1}].$$

Consistency test with an initially constant q_0

Results from LKM
Deviation $q - q_0$ at the simulation end time.



CSLAM-SW: conservative and consistent solver

The scheme is designed to:

1. maintain conservation and consistency
2. require a single solve of a linear Helmholtz equation
3. require a single call to CSLAM

Discrete semi-implicit CSLAM-SW continuity equation

$$h^{n+1} = \bar{h}_{\text{exp}}^{n+1} - \frac{\Delta t}{2} [\nabla_{\text{eul}} \cdot h_{\text{exp}}^{n+1} \mathbf{v}^{n+1} - \nabla_{\text{lag}} \cdot h_{\text{exp}}^{n+1} \tilde{\mathbf{v}}^{n+1}] + \frac{\Delta t}{2} [\nabla_{\text{eul}} \cdot h^n \mathbf{v}^n - \nabla_{\text{lag}} \cdot h^n \mathbf{v}^n] \frac{\delta A^*}{\Delta A}$$

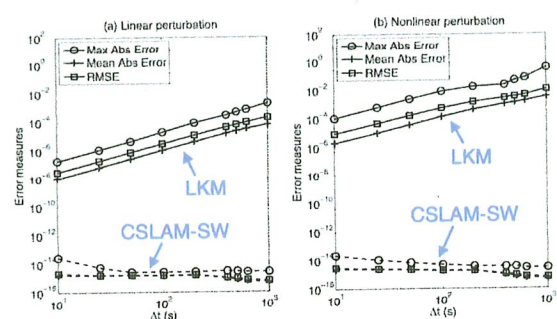
A consistent constituent mass conservation equation

$$\bar{h}q^{n+1} = \bar{h}q_{\text{exp}}^{n+1} - \frac{\Delta t}{2} [\nabla_{\text{eul}} \cdot hq_{\text{exp}}^{n+1} \mathbf{v}^{n+1} - \nabla_{\text{lag}} \cdot hq_{\text{exp}}^{n+1} \tilde{\mathbf{v}}^{n+1}] + \frac{\Delta t}{2} [\nabla_{\text{eul}} \cdot hq^n \mathbf{v}^n - \nabla_{\text{lag}} \cdot hq^n \mathbf{v}^n] \frac{\delta A^*}{\Delta A}$$

(Wong et al. 2013, MWR)

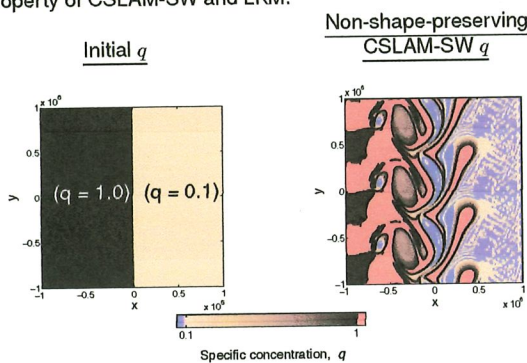
Consistency test with an initially constant q_0

Error is defined as the deviation $q - q_0$ at the simulation end time.



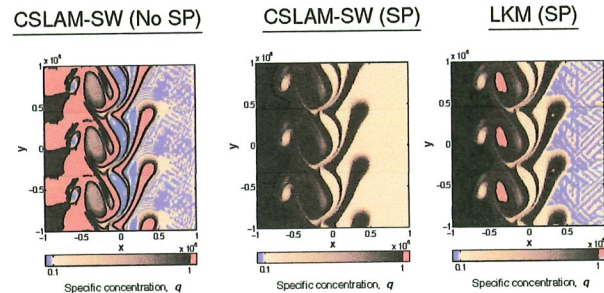
Shape-preservation in CSLAM-SW

Using the Gaussian jet flow, we test the shape-preservation property of CSLAM-SW and LKM.



Shape-preservation in CSLAM-SW

Specific concentration, q
(pink and purple indicate unphysical values)



Shape-preservation is violated in LKM due to inconsistent transport.

Testing of dynamical solvers

Shallow-water systems work well as initial testbeds as a simplified system with only horizontal motion.

Extension to a 2D vertical-slice ($x-z$) fully-compressible nonhydrostatic model.

Governing equations: fully-compressible moist Euler equations

$$\begin{aligned} \frac{du}{dt} &= -\frac{\pi}{\rho_m} \gamma R_d \frac{\partial \Theta'_m}{\partial x} + F_u \\ \frac{dw}{dt} &= -\frac{\pi}{\rho_m} \gamma R_d \frac{\partial \Theta'_m}{\partial z} - \frac{\Delta t}{\rho_m} [g \tilde{\rho}_d \frac{\pi'}{\pi} - g \rho'_m] + F_w \\ \frac{\partial \Theta_m}{\partial t} + \nabla \cdot (\Theta_m \mathbf{v}) &= F_\Theta \\ \frac{\partial \rho_d}{\partial t} + \nabla \cdot (\rho_d \mathbf{v}) &= 0 \\ \frac{\partial Q_j}{\partial t} + \nabla \cdot (Q_j \mathbf{v}) &= F_{Q_j} \end{aligned}$$

where $\pi = (p/p_0)^\kappa$ is the Exner function, $\kappa = R_d/C_p$, $\gamma = c_p/c_v = 1.4$, $R_d = 287 \text{ J kg}^{-1} \text{ K}^{-1}$, $c_p = 1003 \text{ J kg}^{-1} \text{ K}^{-1}$, and $g = 9.81 \text{ m s}^{-2}$. The flux variables are given as

$$\Theta_m = \rho_d \theta_m \quad \text{and} \quad Q_j = \rho_d q_j,$$

where q_j are the mixing ratios of moist species, such as water vapour, cloud water, rain water, etc.

$$u_A^{n+1} = \left[u - \frac{\Delta t}{2} \frac{\pi}{\rho_m} \gamma R_d \delta_x \Theta' \right]_d^n + \Delta t (F_u)_d^n - \frac{\Delta t}{2} \frac{\pi^n}{\rho_m} \gamma R_d \delta_x \Theta_A'^{n+1}$$

$$w_A^{n+1} = \left[w - \frac{\Delta t}{2} \frac{\pi}{\rho_m} \gamma R_d \delta_z \Theta' \right]_d^n + \frac{\Delta t}{\rho_m^n} [g \tilde{\rho} \frac{\pi'}{\pi} - g \tilde{\rho}_m]_{d/2}^{n+1/2} + \Delta t (F_w)_d^n - \frac{\Delta t}{2} \frac{\pi^n}{\rho_m} \gamma R_d \delta_z \Theta_A'^{n+1}$$

$$\Theta_m^{n+1} = \Theta_{m,\exp}^{n+1} - \frac{\Delta t}{2} [\nabla_{\text{eul}} \cdot (\Theta_{m,\exp}^{n+1} \mathbf{v}'^{n+1})] + \frac{\Delta t}{2} [\nabla_{\text{eul}} \cdot (\Theta_m^n \mathbf{v}'^n)] \frac{\delta A^*}{\Delta A} + \Delta t (F_{\Theta_m})_d^n$$

$$\rho_d^{n+1} = \rho_{d,\exp}^{n+1} - \frac{\Delta t}{2} [\nabla_{\text{eul}} \cdot (\rho_{d,\exp}^{n+1} \mathbf{v}'^{n+1})] + \frac{\Delta t}{2} [\nabla_{\text{eul}} \cdot (\rho_d^n \mathbf{v}'^n)] \frac{\delta A^*}{\Delta A}$$

$$Q_j^{n+1} = Q_{j,\exp}^{n+1} - \frac{\Delta t}{2} [\nabla_{\text{eul}} \cdot (Q_{j,\exp}^{n+1} \mathbf{v}'^{n+1})] + \frac{\Delta t}{2} [\nabla_{\text{eul}} \cdot (Q_j^n \mathbf{v}'^n)] \frac{\delta A^*}{\Delta A} + P$$

(Wong et al., 2013, *in prep.*)

Helmholtz equation:

$$-\left(\frac{\Delta t}{2}\right)^2 \gamma R_d \left[\delta_x (\Theta_{m,\exp}^{n+1} \frac{\pi^n}{\rho_m^n} \delta_x \Theta_m'^{n+1}) + \delta_z (\Theta_{m,\exp}^{n+1} \frac{\pi^n}{\rho_m^n} \delta_z \Theta_m'^{n+1}) \right] + \Theta_m'^{n+1} = R_\Theta - \frac{\Delta t}{2} [\delta_x (\Theta_{m,\exp}^{n+1} R_u) + \delta_z (\Theta_{m,\exp}^{n+1} R_w)]$$

R_u , R_w , and R_Θ represent the known terms in the x - and z -momentum eqns and the theta equation.

Compute u^{n+1} and w^{n+1} using Θ'^{n+1} .

Use prescribed winds to solve for ρ_d^{n+1} and Q_j^{n+1} .

Summary

In this presentation, we have looked at:

- Traditional semi-Lagrangian transport schemes
 - trajectory computation
 - grid-point interpolation
- Conservative semi-Lagrangian transport schemes
 - cell-integrated version, CSLAM
- Conservative semi-Lagrangian semi-implicit solvers
 - semi-Lagrangian discretization for advection
 - implicit method to resolve fast-propagating waves
 - Helmholtz equation
 - conservative tracer transport; numerical consistency
 - example solvers:
 - 1) shallow-water 2) fully-compressible nonhydrostatic

The End

References I

- Durran, D.R. (2010)
Numerical methods for fluid dynamics – with applications to geophysics.
Springer, 2nd edition, 516 pp.
- Harris, L.M., P.H. Lauritzen, and R. Mittal (2011)
A flux-form version of the conservative semi-Lagrangian multi-tracer transport scheme (CSLAM) on the cubed sphere grid. *J. Comp. Phys.*, 230, 1215–1237.
- Laprise, J.P.R. and Plante, A (1995)
A class of semi-Lagrangian integrated-mass (SLM) numerical transport algorithms. *Mon. Wea. Rev.*, 123, 553–565.
- Lauritzen, P.H., E. Kaas, and B. Machenhauer (2006)
A Mass-Conservative Semi-Implicit Semi-Lagrangian Limited-Area Shallow-Water Model on the Sphere. *M.W.R.*, 134(4), 1205–1221.

References II

- Lauritzen, P.H., R.D. Nair, and P.A. Ullrich (2010)
A conservative semi-Lagrangian multi-tracer transport scheme (CSLAM) on the cubed-sphere grid. *J. Comp. Phys.*, 229, 1401–1424.
- Lin, S.J. and R.B. Rood (1996)
Multidimensional flux-form semi-Lagrangian transport schemes. *Mon. Wea. Rev.*, 124, 2046–2070.
- Nair, R.D. and Machenhauer, B. (2002)
The mass-conservative cell-integrated semi-Lagrangian advection scheme on the sphere. *Mon. Wea. Rev.*, 130, 649–667.
- Robert, A. (1981)
A stable numerical integration scheme for the primitive meteorological equations. *Atmos.-Ocean*, 19, 35–46.
- Robert, A., T. Yee, and H. Ritchie (1985)
A semi-Lagrangian and semi-implicit numerical integration scheme for multilevel atmospheric models. *Mon. Wea. Rev.*, 113, 388–394.

References III

- Staniforth, A. and Côté, J (1991)
Semi-Lagrangian integration schemes for atmospheric models – a review. *Mon. Wea. Rev.*, 119, 2206–2223.
- Wong, M., W.C. Skamarock, P.H. Lauritzen, and R.B. Stull (2013)
A cell-integrated semi-implicit semi-Lagrangian shallow-water model (CSLAM-SW) with conservative and consistent transport. *M.W.R.*, in press.
- Zerroukat, M., N. Wood, and A. Staniforth (2002)
SLICE: A semi-Lagrangian inherently conserving and efficient scheme for transport problems. *Q. J. R. Meteorol. Soc.*, 128, 2801–2820.